

# Self-Assembly of Methylzinc–Polyethylene Glycol Amphiphiles and Their Application to Materials Synthesis\*\*

Sebastian Polarz,\* Romy Regenspurger, and Jürgen Hartmann

Amphiphilic molecules have proven to be of extraordinary value because they bear the potential to bridge the molecular scale and the nanoscale. They are characterized by two linked molecular parts, which have different solvent compatibilities. When used with a solvent that is compatible with only one of the molecular regions, self-assembly into higher organized structures, such as micelles and lyotropic phases, takes place. Amphiphiles are used in numerous ways: as detergents, for the stabilization of colloidal particles, and even for the preparation of nanoporous materials, to name only a few.<sup>[1]</sup> Classical examples of amphiphiles are surfactants containing a hydrophilic head group (for instance, cationic ammonium) and a long hydrophobic alkyl chain. As a result of the chemical “simplicity” of the head group, classical amphiphiles are rather restricted in expressing additional functional properties. A tempting strategy to extend the functional spectrum of amphiphiles is to equip them with a metal. Some examples of metal-containing amphiphiles exist already in the emerging field of metallomesogens.<sup>[2]</sup> Metals were either introduced as counterions to the head group, or the head group itself contained a multidentate ligand capable of binding to certain metal cations (Werner complexes). Amphiphiles with organometallic head groups and their self-assembly behavior have not yet been reported.

A fascinating perspective of metallomesogens is that the metal could represent a source for the synthesis of an inorganic material. Generally, two sources are used (materials precursor plus structure-directing agent) for the preparation of many nanostructured inorganic materials,<sup>[3]</sup> but metal-containing amphiphiles bear the potential that their self-organization properties could be combined with precursor chemistry in a one-pot approach. Metallomesogens have been

used for the synthesis of nanostructured inorganic materials only rarely.<sup>[4]</sup> There are reports about the covalent anchoring of an alkoxysilane fragment ( $-\text{Si}(\text{OR})_3$ ) to a long alkyl chain through hydrolytically stable Si–C bonds.<sup>[5]</sup> The alkoxysilane fragment fulfills two functions: it becomes the hydrophilic head group after hydrolysis of the silyl ethers, thus inducing the self-organization of a liquid-crystalline phase, and it forms the silicate as a result of polycondensation. To the best of our knowledge, other reports describing the preparation of nanoporous metal oxides from metallic amphiphiles do not exist.

We became interested in the subject of organometallic amphiphiles in the course of our recent studies of a versatile precursor system for the preparation of various zinc oxide (ZnO) materials.<sup>[6,7]</sup> These ZnO precursors are organometallic oxo cluster compounds containing  $\text{ZnCH}_3$  groups and a central “ $\text{Zn}_4\text{O}_4$ ” heterocubane core (see Supporting Information).<sup>[6]</sup> Our initial idea was to prepare a new metallomesogen by attaching a long organic chain to the zinc-oxo cluster core (Supporting Information). As a result of the shielding of the zinc-oxo core with alkyl groups, polar polyethylene glycol (PEG) was selected as a side chain. At the same time the amphiphile should be able to afford a nanostructured ZnO material. The synthesis of the  $\text{Zn}_4\text{O}_4$  heterocubane is simple:<sup>[6,7]</sup> dimethylzinc ( $\text{ZnMe}_2$ ) is reacted with an equimolar amount of a low-molecular-weight alcohol ROH (R: e.g., isopropyl) in anhydrous toluene to afford  $[\text{MeZnOR}]_4$  tetramers in quantitative yield. Therefore, the first attempt to prepare the desired amphiphiles  $[(\text{MeZn})_4(\text{OR})_3\text{OPEG}]$  was to conduct the reaction  $\text{ZnMe}_2 + 0.25\text{PEG}_n + 0.75\text{ROH} \rightarrow ?$ , with  $\text{PEG}_n = \text{HOEt}(\text{OEt})_n\text{OX}$  (X: end groups, OMe, or H;  $n = 400$ , average molecular mass in  $\text{g mol}^{-1}$ ). However, the workup of the reaction showed that the latter approach was too simple. Instead of  $[(\text{MeZn})_4(\text{OR})_3\text{OPEG}]$ , two compounds were isolated: the “normal” heterocubane  $[\text{MeZnOR}]_4$  containing no  $\text{PEG}_n$  and a gel-like substance. In further experiments it was found that the gel results from the reaction of  $\text{ZnMe}_2$  solely with  $\text{PEG}_n$  (Figure 1).

In the following, we concentrate on this gel, termed  $[\text{MeZnOPEG}_{400}]$ . Its molecular-scale structure was characterized, the self-organization on different length scales was studied, and its ability to form ZnO materials was examined.

The gel (Figure 1) was isolated and dried in vacuo. The drying led to a significant shrinkage, which indicates that the material was highly swollen in the initial state. The molecular structure of the solvent-free material was characterized by using a combination of FTIR spectroscopy, NMR spectroscopy, and MALDI-TOF mass spectrometry (MS). The solid-state  $^{13}\text{C}$  NMR spectrum (Figure 2a) is characterized by only two signal groups: besides the ether groups from the PEG

[\*] Dr. S. Polarz, Dipl.-Chem. R. Regenspurger  
Department of Chemistry  
University of Konstanz  
78547 Konstanz (Germany)  
Fax: (+49) 7531-884406  
E-mail: sebastian.polarz@tu-berlin.de

Dr. J. Hartmann  
Max-Planck Institute of Colloids and Interfaces  
Research Campus Golm  
14424 Potsdam (Germany)

[\*\*] This work was funded by the German Science Foundation (DFG) in the framework of an Emmy-Noether research grant. Prof. M. Driess is gratefully acknowledged for his generous support. We thank Dr. B. Smarsly for the small-angle X-ray scattering measurement and R. Breuckmann for the MALDI-TOF mass spectrometry measurements.

Supporting information for this article is available on the WWW under <http://www.angewandte.org> or from the author.

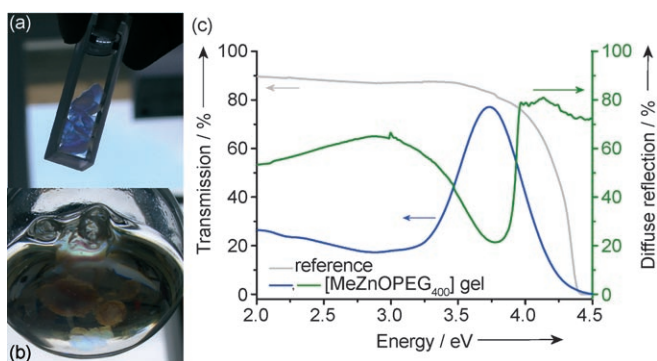


**Figure 1.** Optical properties of the  $[\text{MeZnOPEG}_n]$  gels ( $n = 400$ ). a) Photographic image of the material in transmission mode, b) photographic image of the gel from a different angle, and c) UV/Vis spectra.

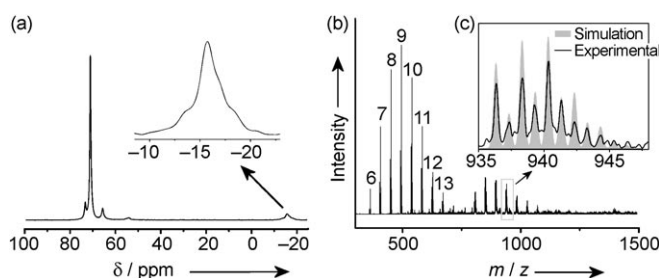


**Figure 2.** a) Solid-state  $^{13}\text{C}$  NMR spectrum and b) MALDI-TOF mass spectrum of the  $[\text{MeZnOPEG}_{400}]$  gel; c) comparison of the isotope pattern correlating to one of the high-mass signals of the dimeric  $[\text{MeZn}_2(\text{OPEG})_2]$  cluster.

( $\delta = 64\text{--}74$  ppm), an additional signal was found at  $\delta = -15.8$  ppm. The latter signal is characteristic for organometallic alkyl zinc-alkoxy moieties (C-Zn-O), and thus the gel contains the expected  $[\text{MeZnOPEG}_{400}]$  units. The NMR results are supported by IR measurements (see Supporting Information). The FTIR spectra of the dried gel and of PEG as a reference are practically identical, but with two important differences: the broad band at  $3345\text{ cm}^{-1}$  found for PEG disappears and a new band at  $668\text{ cm}^{-1}$  appears after reaction with  $\text{ZnMe}_2$ . These differences can be explained by the consumption of PEG-OH groups to form the new  $[\text{MeZnOPEG}_{400}]$  species.

As a result of the polymeric nature of PEG and the gelation process, it was not possible to elucidate the molecular structure of  $[\text{MeZnOPEG}_{400}]$  by crystallographic methods; instead, MALDI-TOF MS was applied (Figure 2b). Two groups of signals are seen in the spectrum: one indicating dinuclear  $[\text{MeZn}_2(\text{OPEG})_2]^+$  clusters (see Figure 2c) and one indicating mononuclear Zn-PEG units (fragmentation products from the ionization process). The MS results indicate that the gel is formed from dimeric molecular building blocks. This finding is in good agreement with the literature, which indicates that the alkyl alkoxides of zinc are likely to form dinuclear clusters for ligands with bulky character.<sup>[8]</sup> In addition, it becomes clear that the  $\text{PEG}_{400}$  was not monodisperse. Besides the PEG chain with  $n \approx 400\text{ gmol}^{-1}$  (nine glycol units), chains with 6–13 units were present as well (Figure 2b). The molecular nature of the  $[\text{MeZnOPEG}_{400}]$

material was further confirmed by adding dry, deuterated toluene to the gel followed by recording of the  $^1\text{H}$  NMR (solution) spectra (shown in Supporting Information). In addition to the signals for PEG ( $\delta = 3.5$  ppm), a signal at  $\delta = -0.32$  ppm (see Supporting Information) is found which is characteristic for  $\text{CH}_3\text{-Zn-OR}$  motifs. The solubility of  $[\text{MeZnOPEG}_{400}]$  proves that the gel is constructed from well-defined, molecular building blocks.

Clearly, the  $[\text{MeZnOPEG}_{400}]_2$  dimers tend to aggregate, and it is necessary to acquire more information about the aggregation process. Polarization microscopy was applied to obtain a first impression (see Supporting Information). Between crossed polarizers  $[\text{MeZnOPEG}_{400}]$  appeared birefringent and a texture was seen comparable to those known from classical liquid-crystal phases. This result indicates that the structure of the material is anisotropic at least in one dimension. Therefore, it makes sense to analyze the organization of the material by more refined methods. Its liquid-crystalline nature was supported by small-angle X-ray scattering (SAXS) and transmission electron microscopy (TEM; Figure 3). The SAXS pattern is dominated by a broad reflex

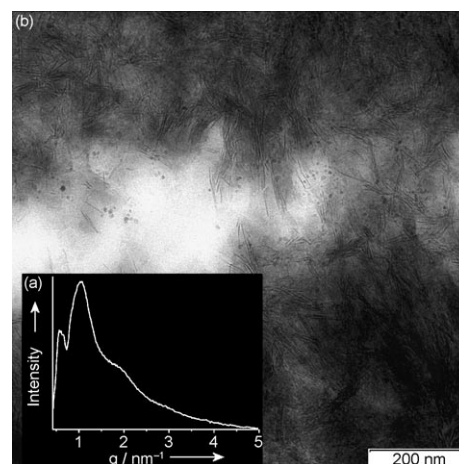


**Figure 3.** a) SAXS pattern and b) TEM image of the dried gel.

at scattering vector  $\mathbf{q} = 1.04\text{ nm}^{-1}$  and two smaller features at  $\mathbf{q} = 1.96$  and  $3.02\text{ nm}^{-1}$ . The data correlate well to a lamellar phase with a periodicity of  $d_{100} \approx 6.04\text{ nm}$ . Next, the material was embedded in an epoxide resin and ultrathin sections were prepared by ultramicrotomy for TEM sample preparation. The TEM measurement supports the conclusions made from SAXS: a self-assembled structure is seen which in many parts resembles a lamellar phase with an average interlattice spacing of  $d_{100} \approx 5.8\text{ nm}$ .

The fact that the  $[\text{MeZnOPEG}_{400}]_2$  dimers aggregate not to disordered structures but to periodic assemblies indicates that they possess amphiphilic properties. It is known from the chemistry of alkyl alkoxides of zinc that the “ZnO” cluster core is shielded by the organic ligands to afford a hydrophobic entity that is readily soluble in apolar solvents such as toluene. On the other hand,  $\text{PEG}_n$  is well known to be more compatible with polar solvents and ultimately water. Therefore, it is reasonable to expect amphiphilic behavior from the

dimers. Molecular modeling studies performed on the lamellar phase lead to an expected periodicity of  $d \approx 5.7$  nm, which is in good agreement with the SAXS and TEM data.

Notably, the amphiphiles described are different from classical amphiphiles, not only because of their organometallic character but also because, unlike surfactants, they possess a nonpolar head group and a polar side chain. However, in analogy to classical amphiphiles that exhibit a complex self-organization behavior when a polar solvent is added, similar phenomena can be expected for the  $[\text{MeZnOPEG}_{400}]_2$  dimers when an apolar solvent is applied. It has already been mentioned that the synthesis in toluene affords solvent-swollen gels; these have a characteristic blue color that is seen when the material is held against the light (Figure 1 a), but from a different angle the gel appears green (Figure 1 b). The occurrence of color is very surprising, as the material does not contain any chromophore. PEG is an aliphatic compound and  $\text{Zn}^{2+}$  is a  $d^{10}$  system. The phenomenon was investigated further by using UV/Vis spectroscopy in the transmission and diffuse reflectance modes (Figure 1 c). Interestingly, the transmission and diffuse reflectance spectra “reflect” each other, which indicates that there is essentially no absorption, only transmission and reflection. Therefore, the described phenomenon can only be explained if the  $[\text{MeZnOPEG}_{400}]$  material contains some sort of an optical grating with periodicities similar to the wavelength of visible light.<sup>[9]</sup>

The investigation of the construction of the gels on even greater length scales became necessary. By measuring the volume ( $V$ ) of one piece of wet gel with a pycnometer, it was possible to determine the porosity  $P = V_{\text{toluene}}/V_{\text{gel}} = 48\%$  of the initial wet gels. Clearly, the  $[\text{MeZnOPEG}_{400}]$  gel is a highly porous system in the wet state. Under conditions of normal drying, that is, vacuum removal of the solvent, the pore system breaks down. However, a facile way to remove the pore fluid without destroying the morphological structure is supercritical drying with carbon dioxide.<sup>[10]</sup> The supercritically dried material could be analyzed by scanning electron microscopy (SEM; see Figure 4 b). A macroporous material is seen,

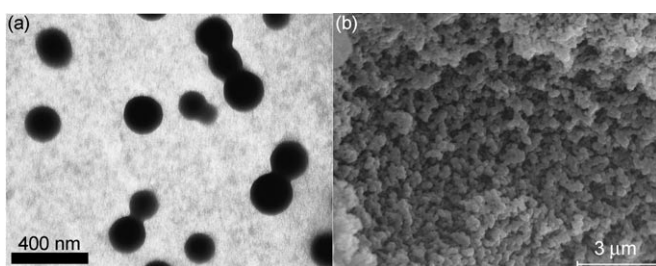


**Figure 4.** a) TEM image of a sample taken in the initial stage of material formation, and b) SEM image along an edge of the supercritically dried  $[\text{MeZnOPEG}_{400}]$  gel.

constructed from the packing of individual, spherical building blocks with an average diameter of 180–200 nm. Energy-dispersive X-ray (EDX) measurements (see Supporting Information) prove that the spheres contain only the elements Zn, C, and O, as expected for  $[\text{MeZnOPEG}_{400}]$ , and the packing of the spherical building blocks explains the unusual

optical properties. An approximation based on a combination of Bragg’s and Snell’s laws allows the optical properties of periodic structures to be estimated;<sup>[11]</sup>  $\lambda$  is proportional to  $2d_{hkl}$ . Clearly, the dimensions of the  $[\text{MeZnOPEG}_{400}]$  “grating” correlate well to the observed optical properties (Figure 5). To further support the formation mechanism of

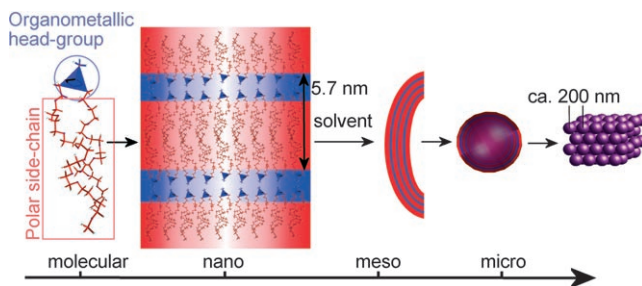


**Figure 5.** Mechanism of hierarchical self-organization for the  $[\text{MeZnOPEG}_n]$  materials starting with dimers at the molecular scale (image on the far left), which assemble into lamellar structures. In contact with toluene, curvature is enforced which leads to large spherical aggregates that finally pack into microscopic domains (image on the far right).

this material, a sample was taken from the reaction mixture directly after warming to room temperature but prior to gelation (see Experimental Section). After filtration through a 450-nm-pore filter, TEM (Figure 4 a) and dynamic light scattering (DLS) measurements (see Supporting Information) were performed. In TEM fairly uniform, spherical particles with an average diameter of ca. 200 nm were found. This result was supported by the DLS measurements, thus indicating that the dispersions contain particles with an average hydrodynamic radius of 102 nm.

It is now possible to propose a reasonable mechanism for the aggregation process of the  $[\text{MeZnOPEG}_{400}]$  material (Figure 5). The reaction of  $\text{ZnMe}_2$  with  $\text{PEG}_n$  affords  $[\text{MeZnOPEG}_n]_2$  dimers. These dimers possess amphiphilic characteristics comparable to those of double-tailed surfactants, with the difference that the head group is nonpolar and the side chain is polar. First, lamellar liquid-crystal-like domains are formed. It is also known from double-tailed surfactants that they tend to form vesicular structures in contact with solvents.<sup>[12]</sup> Similar processes are responsible for the formation of the 200-nm-diameter  $[\text{MeZnOPEG}_{400}]$  spheres. Finally, because of their uniform size, the spheres aggregate into a densely packed structure (Figure 5). Even for classical amphiphiles, such a hierarchical self-assembly process has been documented only rarely. The aggregation process ranges entirely from the molecular to the macroscopic scale.

The question remains whether the dimeric alkyl zinc alkoxide entity in the  $[\text{MeZnOPEG}_{400}]$  material can also be used for the formation of ZnO, in analogy to the mentioned heterocubanes  $[\text{MeZnOR}]_4$ , and whether further information concerning the structure of the resulting ZnO can be encoded because of the PEG.<sup>[6,7]</sup> Therefore,  $[\text{MeZnOPEG}_{400}]$  was applied to the preparation of ZnO in a similar way to the

heterocubanes  $[\text{MeZnOR}]_4$  (see Experimental Section).<sup>[6,7]</sup> A colorless powder was obtained, from which the powder X-ray diffraction (PXRD) pattern (Figure 6a) and FTIR spectrum

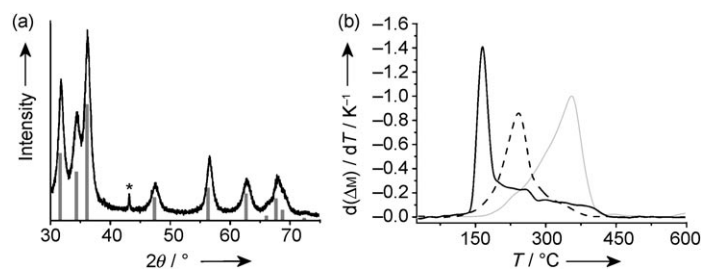


**Figure 6.** a) PXRD data for ZnO derived from  $[\text{MeZnPEG}_{400}]$  (—) and the diffraction pattern of ZnO (PCPDF file 790208) as a reference. The asterisk (\*) denotes a reflex originating from the sample holder. b) Differential thermogravimetric data for the oxidative decomposition of  $\text{PEG}_{400}$  as a reference (gray line), and the  $[\text{MeZnPEG}_{400}]$  material. For the latter, two different heating rates,  $\beta_1 = 1 \text{ K min}^{-1}$  (----) and  $\beta_2 = 30 \text{ K min}^{-1}$  (—), were applied.

(see Supporting Information) were recorded. Both measurements indicate that phase-pure and impurity-free ZnO could be obtained.  $[\text{MeZnOPEG}_{400}]$  is clearly suitable as a ZnO precursor.

As regards the question of whether additional information can be transferred from the molecular to the materials scale, it is reasonable to ask for porosity. The PEG could in principle act as a place holder for the generation of pores. To reach this aim it would be of major importance to remove the PEG at as low a temperature as possible. Thermogravimetric analysis (TGA) was performed to find the optimum conditions. Figure 6b shows the first derivative of the TGA data for better comparison (see also Supporting Information). Pure  $\text{PEG}_{400}$  is characterized by a single mass-loss step with a maximum at  $T = 355^\circ\text{C}$ . The presence of methylzinc leads to a significant change in chemical reactivity. The step of maximum mass loss is shifted to a lower temperature ( $T = 242^\circ\text{C}$ ) for the  $[\text{MeZnOPEG}_{400}]$  material. If, in addition, instead of a low heating rate ( $\beta_1 = 1 \text{ K min}^{-1}$ ) a higher heating rate ( $\beta_1 = 30 \text{ K min}^{-1}$ ) was applied, a further temperature drop to  $T = 164^\circ\text{C}$  and narrowing of the decomposition step were observed.

The porosity of the resulting ZnO material was explored by using  $\text{N}_2$ -physorption analysis (see Supporting Information and Figure 7a,b) and SEM. A mesoporous ZnO material could be prepared with a bimodal pore-size distribution ( $D_{\text{pore}} \approx 4.6$  and  $12.9 \text{ nm}$ ). The material has a Brunauer–Emmett–Teller (BET) surface area ( $S$ ) of  $64.5 \text{ m}^2 \text{ g}^{-1}$ , which is fairly high if one considers the high density of ZnO ( $5.6 \text{ cm}^3 \text{ g}^{-1}$ ). Interestingly, the pore size is in reasonable agreement with the dimension expected from the periodicities in the PEG phase (compare to Figure 5). Even the broad pore-size distribution can be rationalized by the high polydispersity of the  $\text{PEG}_{400}$  (Figure 2b). The porosity of the material can be visualized by SEM images (Figure 7c), in which a strongly textured material is seen. Notably, even the structuration of the  $[\text{MeZnOPEG}]_{400}$  materials on higher length scales can be preserved. The supercritically dried  $[\text{MeZnOPEG}_{400}]$  affords

a zinc oxide with additional, larger features, as seen in the SEM image (Figure 7d). The material consists of globular structures with diameters on the order of  $130 \text{ nm}$ . It is reasonable to assume that the globular ZnO structures result from the transformation of the packed  $[\text{MeZnOPEG}_{400}]$  spheres (compare to Figure 4b). If the PEG chain is really responsible for the formation of pores, one should expect a significant influence of the length of the polymer. To test this hypothesis, ZnO materials were prepared in an analogous manner from  $[\text{MeZnOPEG}_{200}]$  and  $[\text{MeZnOPEG}_{900}]$  (Figure 7a,b). For  $n = 200 \text{ g mol}^{-1}$ , a mesoporous material with an average pore size of  $2.6 \text{ nm}$  and  $S_{\text{BET}} = 67.7 \text{ m}^2 \text{ g}^{-1}$  was obtained. Also here, the pore size is in good agreement with the length of the PEG chains.  $\text{PEG}_{900}$  seems much less able to stabilize a mesoporous framework, as the average pore size ( $D_{\text{pore}} = 27.5 \text{ nm}$ ) and the width of the pore-size distribution (Figure 7a) have both increased and the surface area has decreased ( $S_{\text{BET}} = 29.6 \text{ m}^2 \text{ g}^{-1}$ ). Nevertheless, there is a

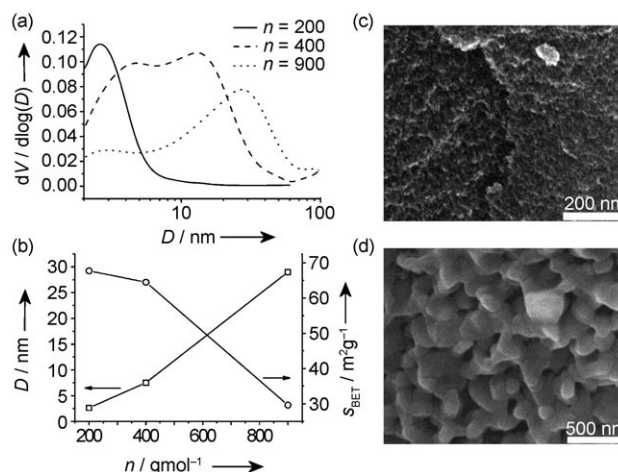


**Figure 7.** a) Barrett–Joyner–Halenda (BJH) pore-size distributions from  $\text{N}_2$ -physorption measurements (see Supporting Information) for three zinc oxide materials obtained from  $[\text{MeZnOPEG}_n]$  with different PEG chain lengths. b) Correlation between PEG chain length, pore size, and BET surface area ( $S_{\text{BET}}$ ) for the prepared materials. c, d) SEM images recorded at different magnifications for ZnO prepared from  $[\text{MeZnOPEG}_{400}]$ .

reasonable correlation between the PEG chain length and the textural properties of the porous ZnO materials (Figure 7b).

Herein, alkyl zinc alkoxide  $[\text{MeZnOPEG}_n]$  materials have been introduced which contain the dimers  $[\text{MeZnOPEG}]_2$ . The dimers represent novel, nonclassical amphiphiles in various respects: their head group is an organometallic oxo cluster; unlike classical surfactants, the head group is non-polar in nature while the side chain is polar; in nonpolar solvents an unusual, hierarchical self-assembly process takes place that spans over several orders of length scale (Figure 5); and finally, it was proven that the amphiphiles are at the same time precursors for nanoporous ZnO, and that the architecture of the amphiphile determines the textural properties of the resulting inorganic oxide.

## Experimental Section

Sample preparation: All chemicals were obtained from Aldrich, carefully dried, and purified prior to use. All reactions were performed under inert-gas conditions in carefully dried glassware using the Schlenck technique. Particular caution is necessary when working with  $\text{ZnMe}_2$  because it spontaneously inflames in contact with air. In a typical synthesis, sodium-dried toluene (100 mL) was cooled to  $-78^\circ\text{C}$  and a solution of  $\text{ZnMe}_2$  in toluene (2 M, 7 mL) was added. An appropriate amount of  $\text{PEG}_n$  was dissolved in toluene (50 mL) and added dropwise under vigorous stirring. An excess of  $\text{ZnMe}_2$  should be used for the preparation of the  $[\text{MeZnOPEG}_n]$  gels. The reaction mixture was warmed to room temperature and stirred for 12 h. At first, clear solutions were obtained, but after 30 min at room temperature a transparent gel started to precipitate slowly from the solution. To obtain the dried gels, toluene (and residual  $\text{ZnMe}_2$ ) was removed by gentle vacuum distillation. All samples were stored under inert conditions (glove box). The mesoporous ZnO materials were prepared by calcining the dried  $[\text{MeZnOPEG}_n]$  gels in oxygen in a tube oven at  $300^\circ\text{C}$  for 1 h. Details of the analytical techniques are given in the Supporting Information.

Received: June 6, 2006

Revised: January 6, 2007

Published online: February 27, 2007

**Keywords:** amphiphiles · metallomesogens · nanoporous materials · self-assembly · zinc oxide

- [1] a) J. S. Beck, J. C. Vartuli, W. J. Roth, M. E. Leonowicz, C. T. Kresge, K. D. Schmitt, C. T. Chu, D. H. Olson, E. W. Sheppard, S. B. McCullen, J. B. Higgins, J. L. Schlenker, *J. Am. Chem. Soc.* **1992**, *114*, 10834; b) D. Zhao, Q. Huo, J. Feng, B. F. Chmelka, G. D. Stucky, *J. Am. Chem. Soc.* **1998**, *120*, 6024.
- [2] a) R. Gimenez, D. R. Lydon, J. L. Serrano, *Curr. Opin. Solid State Mater. Sci.* **2002**, *6*, 527; b) B. Donnio, *Curr. Opin. Colloid Interface Sci.* **2002**, *7*, 371.
- [3] D. Farrusseng, K. Schlichte, B. Spliethoff, A. Wingen, S. Kaskel, J. S. Bradley, F. Schüth, *Angew. Chem.* **2001**, *113*, 4336; *Angew. Chem. Int. Ed.* **2001**, *40*, 4204.
- [4] A. Taubert, *Angew. Chem.* **2004**, *116*, 5494; *Angew. Chem. Int. Ed.* **2004**, *43*, 5380.
- [5] a) Q. Huo, D. I. Margolese, G. D. Stucky, *Chem. Mater.* **1996**, *8*, 1147; b) A. Shimojima, K. Kuroda, *Angew. Chem.* **2003**, *115*, 4191; *Angew. Chem. Int. Ed.* **2003**, *42*, 4057; c) A. Shimojima, Z. Liu, T. Ohsuna, O. Terasaki, K. Kuroda, *J. Am. Chem. Soc.* **2005**, *127*, 14108; d) E. Ruiz-Hitzky, S. Letaief, V. Prevot, *Adv. Mater.* **2002**, *14*, 439; e) J. J. E. Moreau, L. Vellutini, M. W. C. Man, C. Bied, J. L. Bantignies, P. Dieudonne, J. L. Sauvajol, *J. Am. Chem. Soc.* **2001**, *123*, 7957.
- [6] a) S. Polarz, J. Strunk, V. Ischenko, M. Van den Berg, O. Hinrichsen, M. Muhler, M. Driess, *Angew. Chem.* **2006**, *118*, 3031; *Angew. Chem. Int. Ed.* **2006**, *45*, 2965; b) V. Ischenko, S. Polarz, D. Grote, V. Stavarache, K. Fink, M. Driess, *Adv. Funct. Mater.* **2005**, *15*, 1945; c) S. Polarz, A. Roy, M. Merz, S. Halm, D. Schröder, L. Scheider, G. Bacher, F. E. Kruijs, M. Driess, *Small* **2005**, *1*, 540.
- [7] S. Polarz, F. Neues, M. Van den Berg, W. Grünert, L. Khodeir, *J. Am. Chem. Soc.* **2005**, *127*, 12028.
- [8] M. Driess, K. Merz, S. Rell, *Eur. J. Inorg. Chem.* **2000**, 2517.
- [9] a) C. B. Murray, C. R. Kagan, M. G. Bawendi, *Annu. Rev. Mater. Sci.* **2000**, *30*, 545; b) K. Busch, S. John, *Phys. Rev. E* **1998**, *58*, 3896; c) G. A. Ozin, A. C. Arsenault, *Nanochemistry: A Chemical Approach to Nanomaterials*, Springer, Heidelberg, **2005**.
- [10] N. Hüsing, U. Schubert, *Angew. Chem.* **1998**, *110*, 22; *Angew. Chem. Int. Ed.* **1998**, *37*, 22.
- [11] S. Polarz, B. Smarsly, *J. Nanosci. Nanotechnol.* **2002**, *2*, 581.
- [12] D. F. Evans, H. Wennerström, *The Colloidal Domain*, 2nd ed., Wiley-VCH, Weinheim, **1999**.